

Observation of Methyl Radical Recombination Following Photodissociation of CH₃I at 266 nm by Time-Resolved Photothermal Spectroscopy

Myungkoo Suh,[†] Woogyung Sung, Guosheng Li, Seong-Ung Heo, and Hyun Jin Hwang*

Department of Chemistry, Kyung Hee University, Seoul 130-701, Korea

Received November 12, 2002

A time-resolved probe beam deflection (PBD) technique was employed to study the energy relaxation dynamics of photofragments produced by photodissociation of CH₃I at 266 nm. Under 500 torr argon environment, experimental PBD transients revealed two energy relaxation processes; a fast relaxation process occurring within an acoustic transit time (less than 0.2 μs in this study) and a slow relaxation process with the relaxation time in several tens of μs. The fast energy relaxation of which signal intensity depended linearly on the excitation laser power was assigned to translational-to-translational energy transfer from the photofragments to the medium. As for the slow process, the signal intensity depended on square of the excitation laser power, and the relaxation time decreased as the photofragment concentration increased. Based on experimental findings and reaction rate constants reported previously, the slow process was assigned to methyl radical recombination reaction. In order to determine the rate constant for methyl radical recombination reaction, a theoretical equation of the PBD transient for a radical recombination reaction was derived and used to fit the experimental results. By comparing the experimental PBD curves with the calculated ones, the rate constant for methyl recombination is determined to be $3.3(\pm 1.0) \times 10^6 \text{ s}^{-1} \text{ torr}^{-1}$ at $295 \pm 2 \text{ K}$ in 500 torr Ar.

Key Words : Methyl radical, Recombination, Methyl iodide, Photodissociation, Photothermal spectroscopy

Introduction

Photodissociation dynamics of methyl iodide (CH₃I) has been investigated extensively through many experimental¹⁻¹⁰ and theoretical¹¹⁻¹⁵ works. As a result, methyl iodide has become one of prototypical systems for studying photodissociation dynamics of polyatomic molecules.¹⁶⁻²⁰ The information on the photodissociation dynamics of methyl iodide is useful not only for understanding molecular potentials and geometry but also for various applications such as laser generation,²¹ laser-induced chemistry,^{22,23} and atmospheric photochemistry.^{24,25} After the photodissociation of CH₃I, the resulting photofragments undergo numerous and complicated reactions including excess energy transfers and methyl radical recombination.²⁶⁻²⁸ The methyl radical recombination reaction is of special importance since the reaction is a termination step in pyrolysis and combustion.²⁹ Consequently, the chemical kinetics of methyl radical recombination reaction is critical for elucidating flame propagation and ignition processes. In addition, the methyl radical recombination reaction has been served as a standard reaction in steady-state competitive techniques³⁰ in which the rate constants for reactions including methyl radicals are explored.

Time-resolved photothermal spectroscopy technique is known to be very sensitive and versatile for studying photophysical and photochemical processes in solution and

solid.³¹⁻³³ One of advantages of employing photothermal technique is that the technique can be applied to the system in which optical detection is not feasible, since the technique measures the changes in refractive index induced by the heat released from energy relaxation processes. Consequently, it has been applied to numerous processes with a great success.³⁴⁻⁴⁰ In solution, triplet state reactions of organic molecules³⁴⁻³⁶ and lifetimes of photolysis intermediates³⁷ were studied by means of probe beam deflection method (PBD). Energy transfer and vibrational relaxation in gas phase were measured extensively by thermal lensing (TL)³⁸⁻⁴¹ and PBD⁴² techniques. In addition, the PBD technique was employed to monitor a gas phase chemical equilibrium and condensation reaction.⁴³

Despite the versatility of this technique, only a few studies on energy relaxation dynamics of photofragments utilizing photothermal spectroscopy have been reported.⁴⁴⁻⁴⁷ In the photothermal investigation of radical reactions,^{44,45} composite rate constants for chain propagation reactions and chain termination reactions were obtained. In general, the reactions between photofragments are complicated due to their high reactivity, and therefore, acquiring detailed information about individual process by following the energy relaxation is often formidable. Hence, kinetics on methyl radical recombination reaction has been investigated mostly by monitoring the methyl radical absorption at 216 nm.^{27,48,49}

In the present study, we have investigated the energy relaxation dynamics of CH₃I photodissociated at 266 nm by utilizing a probe beam deflection technique. We found that there are two, fast and slow, relaxation processes for the photofragments. The fast process is assigned to translational-to-translational energy transfer of the photofragments to the

*To whom correspondence should be addressed. Phone: +82-2-961-0298, Fax: +82-2-969-3467, E-mail: hjhwang@khu.ac.kr

[†]Present address: Department of Chemistry, Sungkyunkwan University, Suwon 440-746, Korea

medium. And the slow one is determined to be mainly due to the methyl radical recombination reaction at the experimental condition employed in this study; 0.4~1 torr CH₃I photodissociated with 266 nm laser under 500 torr argon. The excess energy partitioning of CH₃I photofragments was compared with the reported values measured by photofragment translational spectroscopy (PTS) method.⁵⁰ It was found that methyl radical recombination reaction rate constants obtained by fitting the slow relaxation process are in excellent agreement with the values reported previously.^{27,48,49,51}

Experimental Section

Methyl iodide (99%, Aldrich Chemical) was used without further purification. Oxygen free argon was prepared by passing high purity argon (99.9999%, Dongjin Jonghab Gas) through an oxygen scrubber (J&W Scientific, Model 600-1011). All experiments were carried out at room temperature.

A detailed experimental setup for monitoring probe beam deflection was described previously,⁴⁶ and therefore only a brief description will be given here. Figure 1 depicts experimental optical set-up. The pump beam was a 266 nm pulsed laser (~5 ns pulse width and ~9 mm beam diameter) that was the 4th harmonic of a Q-switched Nd:YAG laser (Spectra Physics, GCR-150). Typical pulse energy of the pump beam was 300 μJ/pulse to avoid multi-photon absorption processes. The probe beam was a 632.8 nm CW He-Ne laser (Uniphase Model 1125P) with ~1 mm beam diameter and 5 mW output power. At the center of the sample cell that was omitted for simplicity in Figure 1, the focused probe beam crossed the excitation pump beam at right angle and along the long axis of the line focus of the pump beam. A typical Gaussian beam radius of the pump beam along the z-axis at the crossing point, w_0 was 70 ± 5 μm, and a distance between the center of two beams, z_0 was 40 ± 5 μm. Sample gas pressure was measured with two capacitance manometers (MKS Model 122AA-00010AD and 122AA-01000AD). The probe beam deflection signal monitored by a bicell photodiode was amplified, and then recorded by using a digital oscilloscope (LeCroy

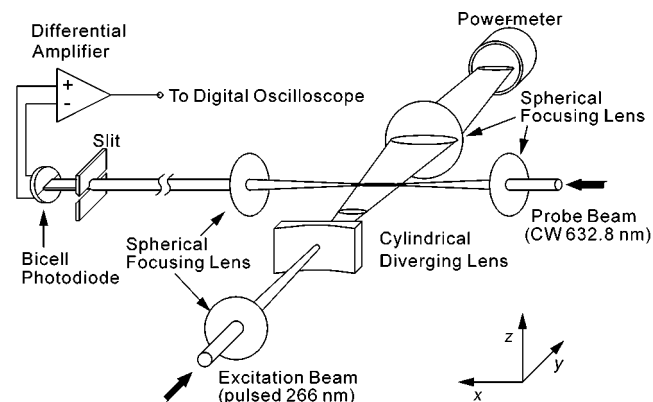


Figure 1. Experimental probe beam deflection (PBD) setup for the time-resolved photothermal spectroscopy study.

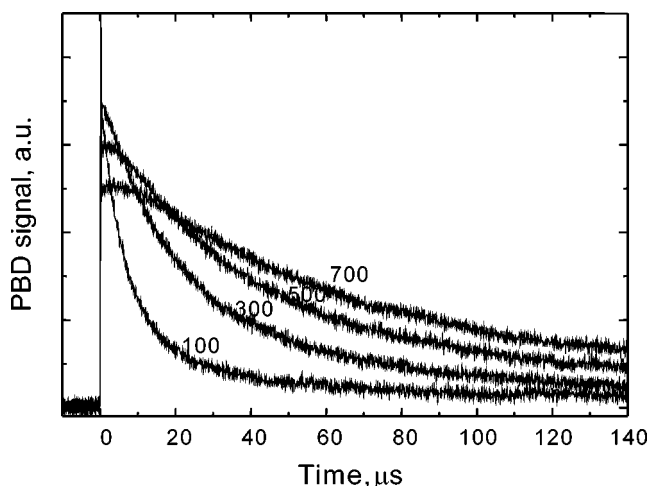


Figure 2. PBD transients for CH₃I and Ar mixtures at various total pressures. The partial pressure of CH₃I was 0.40 torr and the total pressures (in torr) are indicated with curves. The excitation laser pulse energy was 150 μJ/pulse.

Model 9350A).

Experimental PBD transients of CH₃I photofragments under various Ar pressures are depicted in Figure 2. Mainly two processes govern the shape of the PBD transient: a heat releasing process and a thermal diffusion process. The former process affects the early rising part of the PBD curves while the latter process controls the late decaying part. As the argon pressure decreases the PBD curve decays faster since the thermal diffusivity increases. When the thermal decay is too fast, it becomes unfeasible to obtain detailed information about heat releasing processes since the thermal decay dominates over heat releasing. If the thermal diffusion is too slow, the PBD curves become flat and lose their detailed features. As shown in Figure 2, when the argon pressure was 100 torr or 300 torr, the PBD transients were dominated by thermal decay indicating the thermal decay was too fast. At 700 torr argon pressure, not only the signal intensity of the PBD curve diminished due to increased heat capacity of the medium but also the curve became flat. In order to keep the thermal decay slow enough as well as keeping the signal intensity and detailed features, 500 torr argon was chosen as a medium for the experiments.

Results and Discussion

A. Experimental PBD transients of CH₃I photodissociated at 266 nm. Figure 3 shows the PBD transients of CH₃I photodissociated at 266 nm as a function of excitation laser powers. It is noted that not only the signal intensity increases as the excitation laser power increases, but also a significant change in the shape of the curves is observed. This dependence on the excitation laser power indicates strongly that the energy relaxation process(es) is not a first order process in terms of the photofragments. If the relaxation process is a first order process or else it consists of more than one first order process, the shape of the curves must be identical regardless of the excitation laser power since the

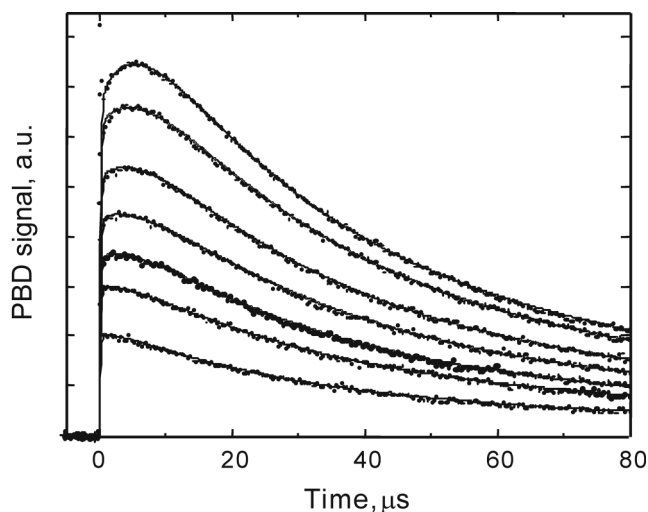


Figure 3. PBD transients for CH₃I and Ar mixture at various excitation laser powers. The excitation laser powers are 104, 141, 164, 197, 227, 274, and 302 μJ/pulse from the bottom. CH₃I pressure was 0.40 torr and total pressure was adjusted to 500 torr with Ar. The solid lines represent the best fit based on Eq. (1).

curve shape only depends on the relaxation time that is constant. We also observed a similar change in the shape of the PBD transient when the CH₃I concentration was varied from 0.4 torr to 1.0 torr (data not shown).

In our previous photothermal deflection spectroscopy study of CF₃I,⁴⁶ we have shown that experimental PBD transients of CF₃I at various excitation laser powers were completely indistinguishable. Only the signal intensity depended linearly on the excitation laser power at the given experimental arrangement. It was concluded for the case of CF₃I that relaxation processes involved in the time domain we used were translational-to-translational (T-T), and vibrational to translational (V-T) energy transfers from photofragments to argon. The differences in excitation energy dependence on PBD curves between CH₃I and CF₃I systems support the presence of a process(es) that is higher than first order reaction with respect to photofragments.

In order to investigate the nature of energy releasing processes that take place after the photodissociation of CH₃I at 266 nm, we have attempted to fit the experimental PBD transients with a theoretical PBD curve that is derived by assuming the heat releasing processes can be described by two first order energy relaxation processes.⁴³ The time-dependent PBD signal, ϕ can be described with two relaxation times, τ_1 and τ_2 , if two heat releasing processes are well separated in time, *i.e.*, one process relaxes much faster than the other:⁴⁶

$$\phi(t, z) = \frac{1}{n} \frac{\partial n}{\partial T} \frac{(-8\alpha E_0 z_0 l f)}{\pi \rho C_p} \frac{[1 - r_1 \exp(-t/\tau_1) - (1 - r_1) \exp(-t/\tau_2)]}{(w_0^2 + 8Dt)^{3/2}} \times \exp\left(\frac{-2z_0^2}{w_0^2 + 8Dt}\right). \quad (1)$$

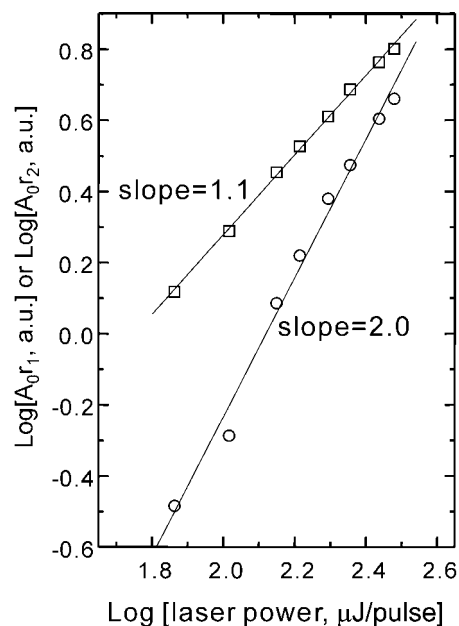


Figure 4. The amount of total released heat observed in PBD transient, A_0 , as a function of excitation laser powers. A_0 is equal to $(1/n)(\partial n/\partial T)((-8\alpha E_0 z_0 l f)/\pi \rho C_p)$ in Eq. (1). Open squares and circles represent the amount of heat contributed from the fast heat releasing process ($A_0 r_1$) and from the slow heat releasing process ($A_0 r_2$), respectively. The solid lines are the linear fitting results for log-log plots. r_1 and r_2 values were obtained by assuming that the observed PBD curves consist of two first order heat releasing processes (see text for details). CH₃I pressure was 0.40 torr and the total pressure was adjusted to 500 torr with Ar.

τ_1 and r_1 are the relaxation time of the fast process and its fractional contribution, respectively, while τ_2 and r_2 are the ones for the slow process. D is the thermal diffusivity of the medium, E_0 is the pump beam energy, and α is the optical absorption coefficient. n is the refractive index, ρ is the density, and C_p is the specific heat at constant pressure. l is the interaction length between the pump and the probe lasers, z_0 is the separation between the centers of pump and probe lasers, and w_0 is an apparent beam waist for a Gaussian-shaped pump beam. f denotes a fractional ratio of excess energy with respect to the total excitation photon energy $h\nu$. For τ_1 , we used 0.2 μs that is the instrumental response time since the actual τ_1 is shorter than the instrument response. For a detailed explanation of the equation given above, please refer to the previous report.⁴⁶

We found that the experimental PBD transients can be fitted relatively well with Eq. (1) in the experimental condition we used, *i.e.* up to 1.0 torr CH₃I and 150 μJ/pulse excitation laser power (see Figure 3). When the excitation laser power and/or CH₃I concentration is higher, we start to observe significant deviation of the experimental PBD curves from the theoretical prediction (data not shown). Nevertheless, r_1 , r_2 and τ_2 values obtained by fitting with Eq. (1) are useful for deducing the nature of the reactions taking place following the photodissociation of CH₃I. As the excitation laser power or CH₃I concentration increases, r_2 value increases while τ_2 value decreases. In Figure 4, the

amount of heat released by fast and slow processes, A_{0r1} and A_{0r2} , respectively, are depicted with respect to the excitation laser power. Note that a striking difference between the slopes in the log-log plot was observed. The slope for the log-log plot of A_{0r1} and excitation laser energy is 1.1 ± 0.1 while the slope for A_{0r2} and excitation energy is 2.0 ± 0.1 . This difference in the slope indicates that the fast and the slow processes observed are quite different in terms of the excitation laser power dependence, and in turn the number of active radicals involved in the process. From the observed slopes, 1.1 and 2.0, it is concluded that a single radical participates in the fast heat releasing process while two radicals are involved in the slow heat releasing process.

The fast relaxation process is easily ascribed to translational-to-translational energy transfer between the photofragments and argon (see discussion given in Ref. 46 for CF₃I). Possible reactions for the slow process are vibrational to translational energy transfer from methyl radical to argon, methyl recombination reaction to produce ethane, and I^* quenching by methyl iodide or methyl radicals. From the reported reaction rate constants^{27,48,49} and experimental findings, the most plausible reaction for the slow process is methyl radical recombination reaction (*vide infra*). The excess energy partitioning of the photofragments after the photodissociation of CH₃I at 266 nm is reported as 34.66: 0.922: 16.3 in kcal/mol (66.8: 1.8: 31.4 in percentile) for $\langle E_t \rangle : \langle E_{int} \rangle : \langle E_e \rangle$.⁵⁰ Here, $\langle E_t \rangle$, $\langle E_{int} \rangle$ and $\langle E_e \rangle$ denote average translational, internal (vibrational and rotational), and electronic energies partitioned into the photofragments upon photodissociation, respectively. Therefore, vibrational to translational energy transfer should be negligible since the vibrational and rotational energies of the photofragments are only 1.8% of the total excess energy. I^* quenching by methyl iodide should not alter the shape of PBD curves at different excitation laser energies since this process involves single radical component, I^* . In addition, I^* quenching rate constant by methyl iodide is reported²⁸ to be $7.0 \times 10^3 \text{ s}^{-1}\text{torr}^{-1}$ which results in hundreds of microseconds as a relaxation time in this experimental condition. On the contrary, I^* quenching by methyl radicals involves two radical components. However, the estimated relaxation time with the reaction rate constant $2.2 \times 10^5 \text{ s}^{-1}\text{torr}^{-1}$,²⁸ falls in milliseconds time scale even in the presence of possible maximum methyl radical concentration ($\sim 4 \times 10^{-3} \text{ torr}$). Consequently, the contribution from I^* quenching by either methyl iodide or methyl radical cannot be observed in the time range (up to 150 μs) we used in the present study.

Since r_1 value corresponds to the contribution from the fast translational to translational energy transfer, it is worth to compare r_1 value with the energy partitioning, 66.8: 1.8: 31.4 in percentile for $\langle E_t \rangle : \langle E_{int} \rangle : \langle E_e \rangle$, obtained by photofragment translational spectroscopy.⁵⁰ As we mentioned earlier, r_1 value decreases as excitation laser power increases. The largest r_1 value observed is $80 \pm 5\%$ at 0.4 torr CH₃I. On the contrary, the largest r_1 value estimated from PTS result is 97% assuming that the contributions from E_e and other chemical reactions are negligible. This substantial discrepancy

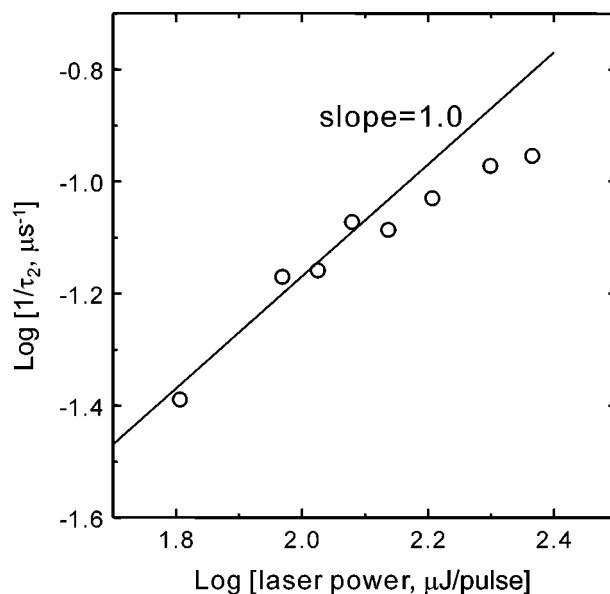


Figure 5. Variation of the slow heat releasing relaxation times with respect to excitation laser power. The relaxation times were obtained by fitting the observed PBD curves with two first order heat releasing processes. CH₃I pressure was 1.0 torr and the total pressure was adjusted to 500 torr with Ar.

in the r_1 value indicates that additional contributions to slow heat releasing process other than vibrational to translational energy transfer from methyl radical to medium exist even in the lowest CH₃I pressure employed in the present study.

Estimated τ_2 value decreases as the excitation laser power increases. Figure 5 shows the log-log relationship between the excitation laser energy and the first order relaxation time for the slow process, τ_2 , that is in several tens of μs . Note that log-log slope between excitation laser power and $1/\tau_2$ is close to 1 suggesting that the slow process is a 2nd order reaction with respect to photofragments. This finding is consistent with the result observed in Figure 4 where the heat released from the slow process depends on the square of the excitation laser power. When the laser power is higher than $\sim 150 \mu\text{J/pulse}$, $1/\tau_2$ value deviates from the unit slope as shown in Figure 5. At this high radical concentration, Eq. (1) fails to fit the PBD transient as mentioned before. Therefore, in order to investigate the kinetics of the photofragments by using PBD transients, a new theoretical equation for PBD signal describing this 2nd order reaction becomes necessary.

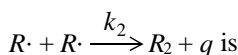
B. Theoretical calculation of PBD transients for a 2nd order radical reaction. We derived a theoretical PBD transient equation for a 2nd order radical reaction to study methyl radical recombination included in the slow heat releasing process. In a crossed-beam setup, when a weakly absorbing sample is exposed to a short excitation pulse, the temperature rise due to a pulsed heat source is described by⁵²

$$T(z, t) = \int_0^t dt' \int_{-\infty}^{\infty} dz' G(z', z, t-t') Q(z', t') \quad (2)$$

where Green's function G is

$$G(z', z, t-t') = \frac{\exp[-(z-z')^2/(4D(t-t'))]}{2\sqrt{\pi D(t-t')}} \quad (3)$$

The heat source term Q for a 2nd order reaction of a type



$$Q(z', t') = k_2 q [N(z', t') / (N(z', t') 2k_2 t' + 1)]^2. \quad (4)$$

Here, q is the heat released per reaction and $N(z', t')$ is the concentration of the excited molecules given by,

$$N(z', t') = \frac{\sqrt{2} \alpha E_0 \exp[-2z'^2 / (w_0^2 + 8D_m t')]}{\sqrt{\pi h \nu l} \sqrt{w_0^2 + 8D_m t'}}. \quad (5)$$

D_m is the molecular diffusivity, k_2 is the bimolecular rate constant defined by $d[R \cdot] / dt = -2k_2 [R \cdot]^2$, and $h\nu$ is the excitation photon energy. By substituting Eq. (5) into (4), the heat source term Q for a 2nd order reaction is obtained as

$$Q(z', t') = k_2 q \left[\frac{c_2 \frac{\exp[-2z'^2 / (w_0^2 + 8D_m t')]}{\sqrt{w_0^2 + 8D_m t'}}}{2c_2 \frac{\exp[-2z'^2 / (w_0^2 + 8D_m t')]}{\sqrt{w_0^2 + 8D_m t'}} k_2 t' + 1} \right]^2 \quad (6)$$

where $c_2 = \frac{\sqrt{2} \alpha E_0}{\sqrt{\pi h \nu l}}$, and $k_2 = 2$ nd order rate constant.

The time-dependent probe beam deflection in z -direction $\phi(z, t)$ is given by:

$$\phi(z, t) = \frac{1}{n} \frac{\partial n}{\partial T} \int_{-\infty}^{\infty} \frac{\partial T}{\partial z} dx = \frac{1}{n} \frac{\partial n}{\partial T} \frac{\partial T}{\partial z} l \quad (7)$$

where n is the refractive index. We calculated the simulated PBD curves, $\phi(z, t)$, based on Eqs. (2) and (7) by use of a numerical integration routine.

In Figure 6, the effects of the 2nd order rate constant and probe beam radius on PBD transients are depicted. It is clearly demonstrated in Figure 6(A) that the increase in rate constant, k_2 , shifts the PBD curve to early time and narrows the width of the curve. As the apparent probe beam radius, w_0 , increases the PBD curves broaden without shifting the peak time. As expected from the Eq. (6), the effect of c_2 is similar to the effect of k_2 on the shape of the PBD curve (data not shown).

C. Methyl radical recombination rate. In order to determine the rate constant for methyl radical recombination reaction, we first estimated the contribution from the slow heat-releasing process by subtracting the contribution from the fast heat-releasing reaction in the experimental PBD transients. Figure 7 shows the subtraction to obtain the PBD curve for the slow heat-releasing process. Simulated fast processes (dashed lines) were used for the subtraction, and subtraction factors were obtained by fitting the experimental PBD curves with Eq. (1). The slow heat-releasing processes at various excitation laser powers that are obtained by the subtraction are shown as dots in Figure 8 with calculated curves in solid lines. It should be noted that the intensity of

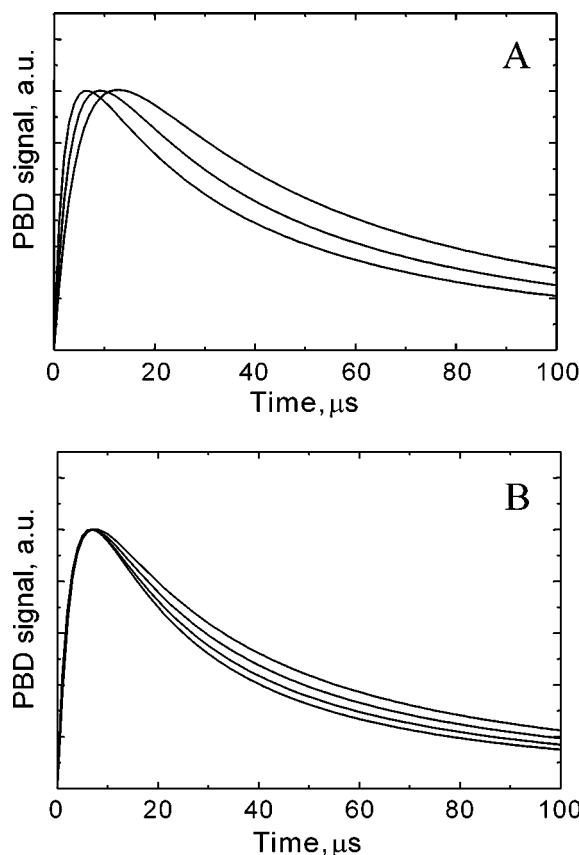


Figure 6. Theoretical PBD curves calculated for various 2nd order bimolecular rate constants, k_2 (A) and for various probe beam radii, w_0 (B). c_2 and z_0 values were set to 3.5×10^{-7} torr-m and $40 \mu\text{m}$, respectively. The bimolecular rate constants, k_2 are 1×10^7 , 2×10^7 , and $4 \times 10^7 \text{ s}^{-1} \text{ torr}^{-1}$ from the left, and w_0 value is set to $80 \mu\text{m}$ (A). w_0 values are $50, 60, 70, 80 \mu\text{m}$ from the top, and k_2 is set to $3 \times 10^7 \text{ s}^{-1} \text{ torr}^{-1}$ (B). All curves are normalized for ease of comparison.

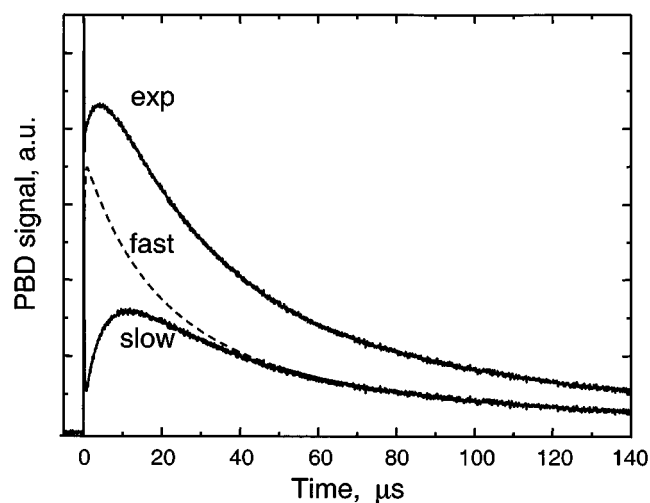


Figure 7. Estimating the PBD transient from the slow heat releasing process. PBD curves for the slow heat releasing process were obtained by subtracting the simulated fast heat releasing process (dashed line) from the experimental PBD curves. Subtraction factors were determined by fitting the experimental curves with Eq. (1).

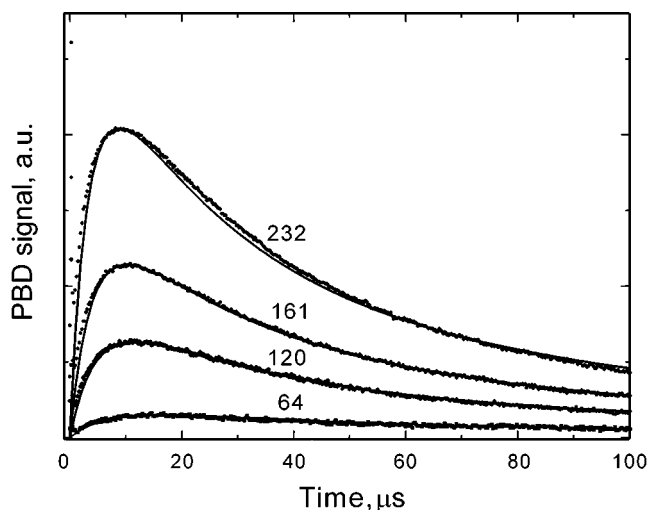


Figure 8. PBD transients for the slow heat releasing processes in CH₃I and Ar mixtures at various excitation laser powers. The excitation powers (in $\mu\text{J}/\text{pulse}$) are indicated with the curves. The solid lines represent the calculated best fit from Eq. (7) by assuming that the slow heat releasing process is the methyl radical recombination reaction (see text for details). For the calculation, w_0 and z_0 values are set to $70\ \mu\text{m}$ and $40\ \mu\text{m}$, respectively. c_2 values are calculated based on Eq. (6) at given excitation powers. The corresponding c_2 (in $\text{torr} \cdot \text{m}$) and k_2 (in $\text{s}^{-1}\text{torr}^{-1}$) values are 2.18×10^{-6} , 3.0×10^6 ; 1.51×10^{-6} , 3.3×10^6 ; 1.10×10^{-6} , 3.0×10^6 ; and 4.81×10^{-7} , 3.7×10^6 from the top, respectively. CH₃I pressure was 1.0 torr and total pressure was adjusted to 500 torr with Ar.

the curves does not depend linearly on excitation laser energies. This non-linear behavior is typical for the reactions involving two radicals, and is consistent with the finding that the amount of heat released from the slow process depends on square of the excitation laser power (see Figure 4). It was also found that the time for the maximum intensity shifted to an earlier time as the excitation laser power increased. This shift in maximum position supports that the slow heat-releasing process is methyl radical recombination reaction since the same shift is observed with the calculated PBD curves for a 2nd order radical reaction.

In Figure 8, the resulting PBD transients for slow heat-releasing processes are compared with the theoretical values, ϕ , calculated by use of Eq. (7). For fitting the experimental curves with theoretical ones, we adjusted the rate constant k_2 in Eq. (7) until the best fit was achieved. c_2 values were calculated for each PBD curve by using $c_2 = \sqrt{2} \alpha E_0 / \sqrt{\pi h \nu l}$ and the experimental parameters used for each measurement. $1.1 \times 10^{-18}\ \text{cm}^2$ was used for the absorption

cross section.⁵³ The solid lines represent the best fit at given experimental conditions. As shown in Figure 8, there is an outstanding agreement between the experimental and the theoretical curves. The average k_2 value obtained by fitting was $3.3 (\pm 1.0) \times 10^6\ \text{s}^{-1}\text{torr}^{-1}$.

In Table 1, previously reported k_2 values are summarized for comparison.^{27,48,49,51} Most comparable k_2 value is $2.3 (\pm 1.0) \times 10^6\ \text{s}^{-1}\text{torr}^{-1}$ that is measured by monitoring the methyl radical absorption in 500 torr argon medium at room temperature.²⁷ Considering the differences in experimental techniques, conditions and errors, our resulting k_2 value is remarkably similar to the ones reported previously. Our resulting k_2 value appears to be only slightly larger than the k_2 values in Table 1. This slight discrepancy is expected since we monitored the time-resolved heat release that is not completely selective for monitoring reactions of methyl radicals. Although the majority of the heat came from the methyl recombination reaction, minor contributions from other processes cannot be entirely ruled out. Fast vibrational to translational energy transfer from methyl radicals to medium can surely contribute to k_2 value slightly (less than a few percent) even at a low methyl radical concentration. The contribution from processes other than methyl radical recombination becomes more discernible at high radical concentrations. As the radical concentration increases, experimental PBD curves starts to deviate from the calculated PBD curves based on methyl radical recombination reaction (see Figure 8) due to other processes occurring at higher radical concentration. Nevertheless, kinetics of the 2nd order radical recombination reaction is monitored successfully by means of probe beam deflection method.

Conclusion

We have shown that the experimental PBD transients of CH₃I photodissociated at 266 nm can be explained by translational to translational energy transfer from photo-fragments to the medium and methyl radical recombination. The theoretical PBD equation for a 2nd order bimolecular process was derived, and was found to describe the experimental PBD curves successfully. We found that the methyl radical recombination reaction dominates up to $\sim 3 \times 10^{-4}$ torr radical concentration. At higher radical concentrations, additional reactions such as I^* quenching and other radical reactions began to contribute significantly. Methyl radical recombination reaction rate constant, k_2 , was obtained easily by fitting the experimental PBD data with theoretical curves.

Table 1. Methyl radical recombination rate constants

Technique	Detection method	Temperature (K)	Pressure (torr)	Rate constant ($\text{s}^{-1}\text{torr}^{-1}$)	References
Laser flash photolysis (193 nm)	216.36 nm radical absorption	298 ± 2	5.4-500, Ar	2.3×10^6	27
Flash photolysis	~ 216 nm radical absorption	293 ± 2	100, Ar	1.5×10^6	48
Flash photolysis	216.4 nm radical absorption	293	200, Ar	2.0×10^6	49
Flash photolysis	150.4 nm radical absorption	room temp.	500-700, He	3.4×10^6	51
Laser flash photolysis (266 nm)	Probe beam deflection	295 ± 2	500, Ar	3.3×10^6	This work

By carefully choosing experimental parameters, this PBD method can be applied successfully to kinetic study of various radical reactions in which optical detection is not feasible.

Acknowledgment. This work was supported by the Korea Research Foundation (Grant No. 1998-001-D00408). M. Suh, G. Li, and S.-U. Heo acknowledge support from the Brain Korea 21 Program of the Ministry of Education, Korea.

References

1. Knee, J. L.; Khundkar, L. R.; Zewail, A. H. *J. Chem. Phys.* **1985**, *83*, 1996.
2. Gedanken, A.; Rowe, M. D. *Chem. Phys. Lett.* **1975**, *34*, 39.
3. Dzvonik, M.; Yang, S.; Bersohn, R. *J. Chem. Phys.* **1974**, *61*, 4408.
4. Sparks, R. K.; Shobatake, K.; Carlson, L. R.; Lee, Y. T. *J. Chem. Phys.* **1981**, *75*, 3838.
5. Barry, M. D.; Gorry, M. D. *Mol. Phys.* **1984**, *52*, 461.
6. Black, F.; Powis, I. *J. Chem. Phys.* **1988**, *89*, 3986.
7. Ogorzalek Loo, R.; Haerri, H.-P.; Houston, P. L. *J. Phys. Chem.* **1988**, *92*, 5.
8. Hall, G. E.; Sears, T. J.; Frye, J. M. *J. Chem. Phys.* **1989**, *90*, 6234.
9. Hess, W. P.; Kohler, S. J.; Haugen, H. K.; Leone, S. R. *J. Chem. Phys.* **1986**, *84*, 2143.
10. Sundberg, R. L.; Imre, D.; Hale, M. O.; Kinsey, J. L.; Coalson, R. D. *J. Phys. Chem.* **1986**, *90*, 5001.
11. Shapiro, M.; Bersohn, R. *J. Chem. Phys.* **1980**, *73*, 3810.
12. Henrikson, N. E. *Chem. Phys. Lett.* **1985**, *121*, 139.
13. Xie, D. Q.; Guo, H.; Amatatsu, Y.; Kosloff, R. *J. Phys. Chem. A* **2000**, *104*, 1009.
14. Hennig, S.; Engel, V.; Schinke, R. *J. Chem. Phys.* **1986**, *84*, 5444.
15. Yabushita, S.; Morokuma, K. *Chem. Phys. Lett.* **1988**, *153*, 517.
16. Lao, K. Q.; Person, M. D.; Xayariboun, P.; Butler, L. J. *J. Chem. Phys.* **1990**, *92*, 838.
17. Guo, H.; Schatz, G. C. *J. Chem. Phys.* **1990**, *95*, 3091.
18. Guo, H. *J. Chem. Phys.* **1992**, *96*, 2731.
19. Gray, S. K.; Child, M. S. *Mol. Phys.* **1984**, *51*, 189.
20. Hermann, H. W.; Leone, S. R. *J. Chem. Phys.* **1982**, *76*, 4766.
21. Kasper, J. V. V.; Parker, H.; Pimentel, G. C. *J. Chem. Phys.* **1965**, *43*, 1827.
22. Choi, Y.-K.; Koo, Y.-M.; Jung, K.-W. *J. Photochem. Photobiol. A: Chem.* **1999**, *127*, 1.
23. Ford, J. V.; Poth, L.; Zhong, Q.; Castleman Jr., A. W. *Int. J. Mass Spectrom.* **1999**, *192*, 327.
24. Lee, A. Y. T.; Yung, Y. L.; Moses, J. J. *Geophys. Res. E*, **2000**, *105*, 20207.
25. Bezdard, B.; Romani, P. N.; Feuchtgruber, H.; Encrenaz, T. *Astrophys. J.* **1999**, *515*, 868.
26. Burde, D. H.; McFarlane, R. A. *J. Chem. Phys.* **1976**, *64*, 1850.
27. Macpherson, M. T.; Pilling, M. J.; Smith, M. J. C. *J. Phys. Chem.* **1985**, *89*, 2268.
28. Palmer, R. E.; Padrick, T. D. *J. Chem. Phys.* **1976**, *64*, 2051.
29. Baulch, D. L.; Duxbury, J. *J. Combust. Flame* **1980**, *37*, 313.
30. Kerr, J. A.; Parsonage, M. J. *Evaluated Kinetic Data on Gas Phase Hydrogen Transfer Reactions of Methyl Radicals*; Butterworths: London, 1976.
31. Laman, D. M.; Falvey, D. E. *Rev. Sci. Instrum.* **1996**, *67*, 3260.
32. (a) Tam, A. C. In *Photothermal Investigations of Solids and Fluids*; Academic Press: New York, 1989; Chap. 1. (b) Barker, J. R.; Toselli, B. M. In *Photothermal Investigations of Solids and Fluids*; Academic Press: New York, 1989; Chap. 5.
33. Braslavsky, S. E.; Heibel, G. E. *Chem. Rev.* **1992**, *92*, 1381.
34. Yeh, S.-R.; Falvey, D. E. *J. Photochem. Photobiol. A: Chem.* **1995**, *87*, 13.
35. Terazima, M.; Azumi, T. *J. Phys. Chem.* **1990**, *94*, 4775.
36. Terazima, M.; Azumi, T. *J. Phys. Chem.* **1990**, *94*, 4775.
37. Robbins, R. J.; Laman, D. M.; Falvey, D. E. *J. Am. Chem. Soc.* **1996**, *118*, 8127.
38. Toselli, B. M.; Walunas, T. L.; Barker, J. R. *J. Chem. Phys.* **1990**, *92*, 4793.
39. Grabiner, F. R.; Siebert, D. R.; Flynn, G. W. *Chem. Phys. Lett.* **1972**, *17*, 189.
40. Bailey, R. T.; Cruickshank, F. R.; Guthrie, R.; Pugh, D.; Weir, I. J. *M. Chem. Phys.* **1987**, *114*, 411.
41. Trevor, P. L.; Rothen, T.; Barker, J. R. *Chem. Phys.* **1982**, *68*, 341.
42. Calasso, I. G.; Delgadillo, I.; Sigrist, M. W. *Chem. Phys.* **1998**, *229*, 181.
43. Sontag, H.; Tam, A.; Hess, P. *J. Chem. Phys.* **1987**, *86*, 3950.
44. Cambron, R. T.; Harris, J. M. *Anal. Chem.* **1995**, *67*, 365.
45. O'Connor, M. T.; Diebold, G. J. *Nature* **1983**, *301*, 321.
46. Suh, M.; Sung, W.; Heo, S.-U.; Hwang, H. J. *J. Phys. Chem. A* **1999**, *103*, 8365.
47. Lee, J. S.; Hwang, H. J. *Bull. Korean Chem. Soc.* **1997**, *18*, 11.
48. van den Bergh, H. E.; Callear, A. B.; Norstrom, R. J. *Chem. Phys. Lett.* **1969**, *4*, 101.
49. James, F. C.; Simons, J. P. *Int. J. Chem. Kinet.* **1974**, *6*, 887.
50. Eppink, A. T. J. B.; Parker, D. H. *J. Chem. Phys.* **1999**, *110*, 832.
51. Bass, A. M.; Laufer, A. H. *Int. J. Chem. Kinet.* **1973**, *5*, 1053.
52. Jackson, W. B.; Amer, N. M.; Boccara, A. C.; Fournier, D. *Appl. Opt.* **1981**, *20*, 1333.
53. Waschewsky, G. C. G.; Horansky, R.; Vaida, V. *J. Phys. Chem.* **1996**, *100*, 11559.